Frontiers in Computing and Intelligent Systems
ISSN: 2832-6024 | Vol. 13, No. 3, 2025

Intelligent Control System for Infrared Hot Air Drying Equipment Based on PLC

Peng Yu [1], Lin Dong [2,*], Cheng Yin [1], Zhenghai He [1], Jiahui Wang [1], Shuang Wang [3]

[1] School of Mechanical Engineering, Xihua University, Chengdu, Sichuan 610039, China
[2] Institute of Modern Agricultural Equipment, Xihua University, Chengdu Sichuan 610039, China
[3] Oriental Hitachi (Chengdu) Electric Control Equipment Co., Ltd., Chengdu Sichuan 611731, China

[*] **Corresponding author**: Lin Dong (Email: lin.dong@mail.xhu.edu.cn)

Abstract: China's agricultural output has consistently ranked among the global leaders in recent years. However, most agricultural products and by-products are characterized by high moisture content and perishability, with improper post-harvest handling leading to significant losses. Drying technology serves as a critical preservation method. Infrared-hot air combined drying, leveraging its dual advantages of penetration heating and energy efficiency, has emerged as a pivotal approach in sustainable drying solutions. Nevertheless, existing equipment faces challenges such as low automation and high energy consumption. To achieve precise temperature control and intelligent regulation in infrared-hot air drying systems, this study developed an intelligent control system based on programmable logic controllers (PLC) using Sichuan Da hong citrus peel as experimental material, addressing key limitations of conventional equipment including poor drying quality, high energy consumption, and insufficient intelligence. The main research contributions and conclusions are as follows.

Keywords: Drying of Dried Tangerine Peel; Intelligent Control System; Infrared Hot Air Drying Technology; Programmable Logic Controller (PLC).

1. Introduction

The market offers various types of drying ovens, with infrared hot air drying ovens standing out by combining the advantages of both infrared radiation and hot air drying to achieve efficient synergy between thermal energy transfer and moisture migration. During the drying process, infrared radiation penetrates the material's surface layer, where molecules absorb thermal energy. This intensifies molecular vibrations, raising internal temperatures and accelerating moisture evaporation[1]. Simultaneously, the hot air system rapidly removes free moisture through forced convection, balancing temperature gradients and effectively addressing the common "dry exterior, moist interior" issue in traditional hot air drying [2]. The core technology lies in dynamically adjusting the energy ratio between infrared and hot air. For instance, high infrared radiation is used in the initial stage to rapidly increase temperature and shorten preheating time; during intermediate stages, hot air disperses moisture to prevent crust formation; while in later stages, low-power infrared combined with hot air prevents material charring [3]. By controlling infrared heating plates and fans via frequency converters, coupled with real-time temperature/humidity feedback, the system can adjust heating power according to material characteristics (e.g., porous structures, heat-sensitive components) to ensure consistent drying quality [4]. Qu Wenjuan et al.[5] found that composite drying reduced drying time by 19.2% and energy consumption by 11.6% compared to single technology when drying fresh walnuts with infrared-hot air. The directional heating of infrared radiation minimizes ineffective heat loss, while the hot air circulation design enhances airflow uniformity [6], making it particularly suitable for drying flaky, granular, or uneven-thickness materials while significantly reducing issues like cracking and deformation. Infrared hot air drying technology demonstrates exceptional performance in applications such as high-moisture fruit and vegetable crisp production, retention of active components in traditional Chinese medicinal materials, and rapid shaping of ceramic green bodies. For instance, in food processing, composite drying not only rapidly removes moisture and preserves coloration but also prevents nutrient loss caused by localized overheating through hot air circulation. When applied to apple slices, this technology effectively suppresses browning, enhances drying efficiency, and improves product quality [7].

2. Composition and Method of Control System Hardware

The infrared hot air drying chamber is structured as shown in Figure 1, with dimensions of 1100mm×680mm×640mm (length×width×height). Both the inner and outer walls feature stainless steel construction, while insulation cotton is filled in the middle to minimize heat loss. A top-mounted axial fan (12) drives hot air circulation within the chamber, effectively reducing energy waste [8]. A PTC heating resistor (10) positioned left of the fan heats the air medium, which continues circulating under the fan's impetus. A graphene infrared heating plate (9) above the material tray enables efficient radiant heating of materials. Temperature sensors (11,13) installed on upper and lower layers monitor internal temperatures in real-time, feeding data to the control system for power adjustment and temperature regulation. Two humidity sensors (14,17) paired with a dehumidification fan maintain chamber humidity. The dehumidifier operates at exhaust vents (16) to prevent humid air from mixing with incoming airflow, while an induced draft fan is installed inside the intake vents (15). Control components on the left side (6) integrate PLC and human-machine interfaces, supporting multi-stage process programming. Users can preset temperature and humidity settings for automated drying, with built-in fault alarms and data logging capabilities.

To mitigate the effects of fan vibration and temperature fluctuations on load cells, a modular design integrating the sensor with housing is implemented. The weight sensor is mounted at the base (7) of the housing, connected to a vibration-absorbing sponge pad at the interface. A connecting rod links the sensor to the material tray (8). During drying, the sensor continuously monitors weight variations in the material. Since moisture content directly affects weight measurements, precise analysis of these data points enables real-time monitoring of moisture changes. The collected information is transmitted to the PLC control system, providing precise data support for optimizing drying parameters and refining processes based on moisture fluctuations [9-15]. Key technical specifications of the drying chamber are detailed in Table 1

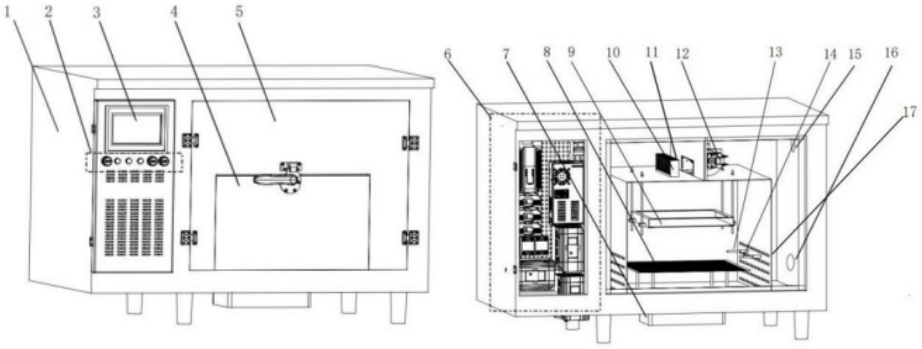

(a) Overall appearance (b) Internal structure

1. Cabinet 2. Control Buttons 3. Touchscreen 4. Material Door 5. Maintenance Door 6. Control Components 7. Weight Sensor 8. Material Tray 9. Graphene Infrared Heating Plate 10.PTC Heater 11. Upper Temperature Sensor 12. Axial Fan 13. Lower Temperature Sensor 14. Inner Humidity Sensor 15. Air Inlet 16. Exhaust Outlet 17. Outer Humidity Sensor

Figure 1. Composition structure of dryer

Table 1. Main technical parameters of drying chamber

number	Characteristic technical parameters	numeric value
1	External dimensions (length × width × height)	1100mm×680mm×640mm
2	Temperature adjustment range	0-130℃
3	Humidity adjustment range	0-100%
4	Graphene infrared panel power	1000W
5	PTC heating resistance power	500W
6	Weighing	0-3kg
7	Internal wind speed	0-3m/s
8	Plate size	40cm×40cm
10	rated voltage	220V
11	aggregate capacity	2000W

2.1. Working Principle of Intelligent Control of Infrared Hot Air Drying Chamber

The infrared hot air drying chamber operates through PLC control and utilizes the principles of infrared radiation and hot air drying, as illustrated in Figure 2.2. During operation, users configure target temperature and humidity parameters via the human-machine interface while activating both infrared heating plates and PTC heating resistors. External air is drawn into the duct system by the right-side induced draft fan. The heating resistors heat air to set temperatures through forced convection, while infrared heating plates above the material tray emit far-infrared radiation. This penetrates material surfaces, activating internal water molecule resonance to generate thermal energy, creating a dual heating effect of external convection and internal radiation. Axial fans drive hot air to form a closed-loop circulation system: heated air is evenly distributed into the drying chamber through the left airflow distribution chamber. After completing heat-moisture exchange with materials, the vaporized moisture returns to the right duct via axial fans for residual heat recovery, minimizing thermal loss. Integrated weighing sensors monitor material mass changes in real-time, dynamically displaying evaporation rates (evaporation=initial mass-current mass). When humidity sensors detect excessive chamber moisture levels, PLC controls activate dehumidification fans and induced draft fans to rapidly expel moisture while replenishing preheated fresh air. This ensures optimal temperature-humidity balance throughout the drying process, achieving energy-efficient collaborative drying.

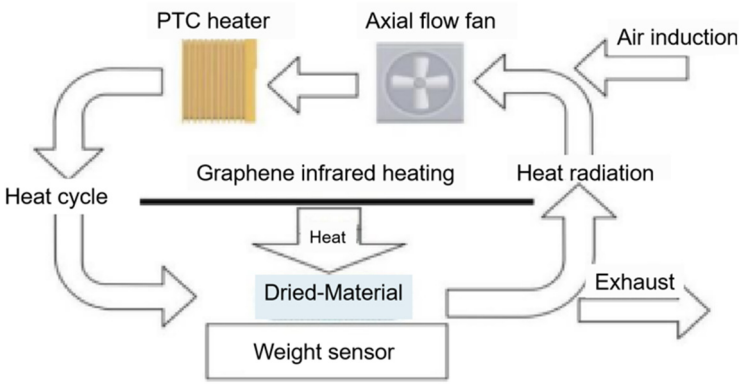

Figure 2. Working principle

The system employs temperature and humidity sensors to monitor real-time environmental conditions within the chamber. A PID control algorithm dynamically adjusts the power supply to the temperature control system, while a PLC manages the humidity control. When evaporation during material drying causes relative humidity to exceed preset thresholds, the system activates dehumidification fans. These high-performance units rapidly expel humid air through exhaust vents while simultaneously introducing fresh air via the ventilation system. This dual-channel airflow mechanism effectively reduces chamber humidity to target levels, with the dehumidification motors automatically deactivating once humidity parameters meet specifications.

2.2. Intelligent Control Hardware System

The infrared hot air drying box control system includes PLC main controller, HMI, temperature sensor, humidity sensor, weight sensor, infrared heating plate, PTC heating resistor, frequency converter, dehumidification fan, axial flow fan and other components.

The control system of the drying chamber uses Mitsubishi FX programmable controller as the main control unit, which enables the start and shutdown of various moving parts through relays and frequency converters. The touchscreen communicates with PLC to monitor the operating status of each actuator unit in real time, displaying information collected by various sensors on the screen.

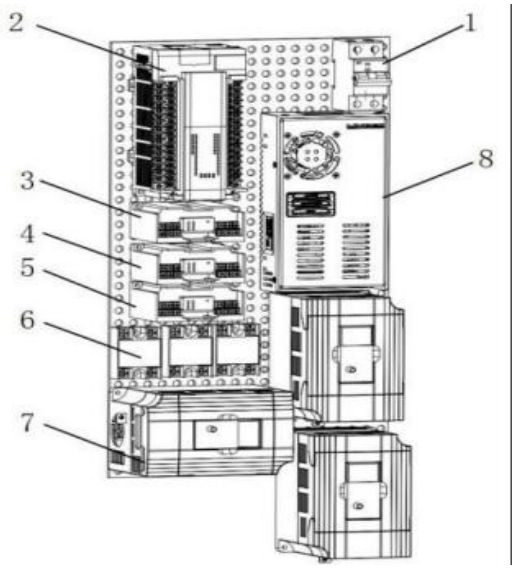

1. Air switch 2. Mitsubishi FX2N PLC 3.TC module 4. DA module 5.AD module 6. Solid state relay7. Inverter 8. Switching power supply

Figure 3. Control cabinet hardware installation diagram

2.3. Hardware Wiring Diagram

According to the requirements of infrared hot air drying chamber control system, the required hardware scheme of the control system is determined. The selected hardware includes PLC and HMI, PLC input/output module, heating and exhaust hardware equipment, etc. The wire bundle color classification of the hardware wiring diagram is shown in Table 2.

Table 2. Hardware diagram wiring harness color

order number	name	pigment
1	battle line	red
2	null line	black
3	DC positive	brown
4	DC negative	black
5	earth wire	olivine
6	PLC import	blue
7	PLC output	yellow

The wiring diagram of the system hardware is shown in Figure 4.

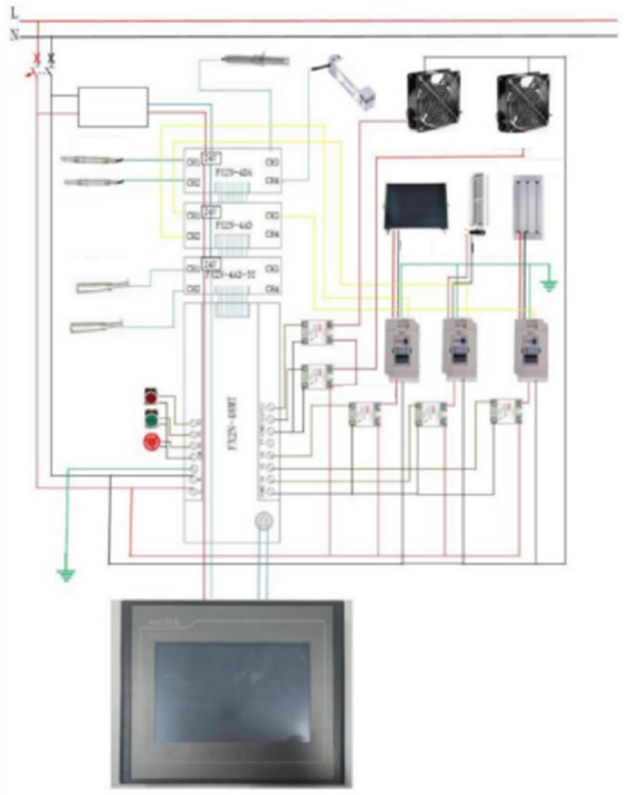

Figure 4. system hardware wiring diagram

2.4. Intelligent Control Software System

In this control system, Mitsubishi FX2N PLC is selected as the core master controller. The main program is developed using GX Works2 software, employing intuitive ladder diagram as the programming language while adopting a modular design philosophy. The system includes: a temperature control program for thermal regulation; a humidity monitoring program for data acquisition; a wind speed control program for airflow regulation; an infrared hot air heating program; a dehumidification control program for motor operation; and a circulation fan control program to ensure stable operation of the circulating fans [16].

The configuration control interface is designed to use Kunlun Tongtai PTC7062Ti touch screen, and the operation interface is built by using MCGSE configuration software.

The control interface selects the Kunlun Tongstate PTC7062Ti touch screen, which is equipped with a 7-inch resistive screen. The design concept of this device is to face the user and divide the control system configuration interface into four sections: user main interface, manual control interface, parameter setting interface and PID control interface.

3. Testing and Analysis

3.1. Tangerine Peel Drying Test Equipment

For this drying experiment, we selected the "Da Hong Pao Citrus" variety of Sichuan Red Orange from its origin in Sichuan Province. The fruits were purchased from a local market, featuring a flat-round shape with smooth, delicate surfaces displaying a deep, uniform orange-red color. Their peels were densely dotted with oil spots and had a loose texture that was easy to peel. The peeling process employed the "Three-Stroke Method": starting from the top of the fruit toward the stem, three longitudinal cuts were made while keeping the stem connected. After the three-stroke peeling technique, the dried fruit peel became known as "Chuan Chen Pi" (Sichuan-aged peel). The experimental materials are shown in Figure 5.

The equipment used in this experiment is the infrared hot air drying box designed in this paper, and the electric constant temperature blower drying box is selected as the comparison. The dried tangerine peel is dried at the same temperature, and the electronic balance is used to measure the weight change of tangerine peel. The model numbers of the equipment used in this experiment are shown in Table 3.

Figure 5. Experimental materials Dahongpao citrus

Table 3. Dried tangerine peel equipment

order number	device name	Model parameters
1	Electric thermal constant temperature fan drying chamber	DHG-9146A accuracy ±1℃
2	electronic balance	FA2204 accuracy 0.1mg
3	Infrared hot air drying chamber	A0001

3.2. Dried Tangerine Peel Test Method

The red tangerine peel is evenly divided into three segments using the "three-cut method", with excess portions trimmed to maintain total weight at 20.5g. Following the Xinhui Citrus Peel Production Standard DB4407/T 70-2021, the moisture content must not exceed 13% [17]. The peel's weight is measured every 20 minutes. When the weight approaches 6.78g, shorten the measurement time; if it falls below 6.6g, stop drying immediately.

During the drying process, increased temperature significantly enhances the potential energy of internal moisture migration in materials, accelerating the removal rates of bound and free water to reduce drying time. However, when temperatures exceed critical thresholds, volatile essential oils are released, causing rapid component

evaporation. This triggers thermal degradation reactions in flavonoid active substances and may induce Maillard reactions in carbohydrates, forming a dense surface layer that impedes internal moisture transfer. Conversely, excessively low drying temperatures may induce enzymatic browning reactions, promoting continuous action of polyphenol oxidases. Prolonged drying also increases microbial contamination risks and leads to irreversible transformation of terpenoid substances before the characteristic aroma of dried tangerine peel is formed. Based on previous research and considering that the optimal drying temperature for Xinhui dried tangerine peel typically does not exceed 45°C, this study established three temperature gradient experiments at 30°C, 35°C, and 40°C. Comparative drying tests were conducted using an electrically heated constant-temperature ventilated dryer and a specially developed infrared hot air dryer.

3.3. Analysis of Test Results

(1) Drying time analysis

According to the test data, the dry base moisture content is calculated by formula 4.10 as shown in Figure 6.

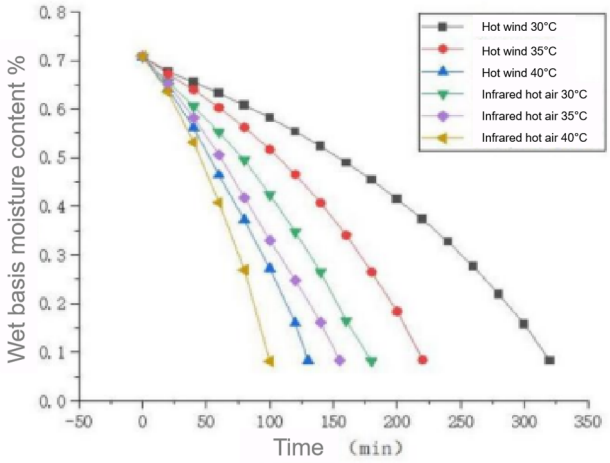

Figure 6. Moisture content of dry foundation

The test moisture content was achieved through dry drying (≤8.4%). The drying times were: hot air 30°C at 320 minutes; hot air 35°C at 220 minutes; hot air 40°C at 130 minutes; infrared hot air 30°C at 180 minutes; infrared hot air 35°C at 155 minutes; infrared hot air 40°C at 100 minutes. Under identical temperature conditions, the infrared hot air dryer reduced the required drying time by 43.75%,29.54%, and 23.07% respectively.

The drying time of both is shortened when the temperature rises, and the time required by infrared hot air drying at the same temperature is less. The drying rate of the designed infrared hot air drying equipment is higher than that of electric heat constant temperature blower drying box.

(2) Coefficient of uneven drying

Fresh fruit peels were cut into 5mm×5mm cubes using scissors, with identical-sized samples obtained through the five-point sampling method (as shown in Figure 7). The pre-dried mass of these 5mm×5mm cubes was measured and averaged to obtain a value of 0.05g. Based on the average moisture content, the absolute dry weight of each cube was calculated as 0.019g. After drying, the dried fruit peel cubes were positioned and weighed, with detailed records documented in Table 3.2. The parameter MCave represents the average moisture content of the fruit peel where each cube was located.

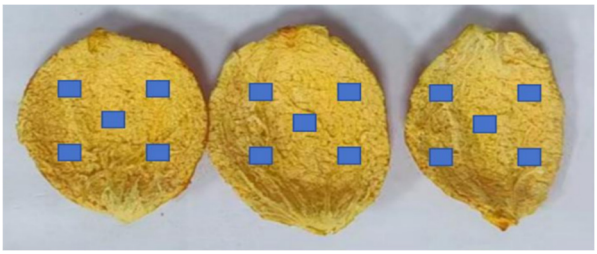

Figure 7. Fruit peel sampling points

As shown in Table 4, both hot air drying and infrared drying exhibited increased non-uniformity coefficients with temperature increases. At identical temperatures, infrared drying demonstrated 55.45%, 49.18%, and 52.12% reductions in non-uniformity coefficients respectively. The significant increase in hot air drying's coefficient stems from its heat exchange mechanism: heat gradually transfers from material surfaces to interiors through thermal convection, causing surface temperatures to exceed internal moisture levels. This results in rapid surface drying without adequate internal moisture migration, leading to substantial unevenness. In contrast, infrared drying utilizes radiant heating to generate internal molecular vibrations, creating localized heat sources that penetrate material interiors. This approach reduces temperature differential effects, significantly improving drying uniformity. Experimental data confirms that the designed infrared hot air drying chamber achieves higher material uniformity compared to electrically heated constant-temperature drum dryers.

Table 4. Coefficient of dryness inhomogeneity

parameter	Hot air 30℃	hot-blast air 5℃	Hot air 40℃	Infrared hot air 30℃	Infrared hot air 35℃	Infrared hot air 40℃
MCmax	9.76%	10.61%	12.26%	9.33%	9.33%	10. 19%
MCmin	5.74%	5.27%	5.74%	7.57%	6.67%	7. 12%
MCave	8.26%	8.40%	8.26%	8. 12%	8.26%	8. 12%
nonuniformity coefficient CN	48.69%	63.56%	78.91%	21.69%	32.30%	37.78%

(3) Citrus peel shrinkage rate

The volume before and after drying was calculated by the drainage method, and the average volume of fresh tangerine peel 20.5g was 22ml, as shown in Figure 8.

The experimental results are shown in Table 3.2. The overall shrinkage rate of infrared hot air heating was lower than that of conventional hot air drying. At the same temperature, the shrinkage rates under infrared drying

conditions decreased by 5.57%,4.92%, and 5.26% respectively. The infrared panel emitted radiation more uniformly, ensuring both the surface and interior of the dried citrus peel received consistent thermal exposure. This resulted in more uniform drying speeds across different sections, leading to relatively even shrinkage and a significantly reduced overall shrinkage rate.

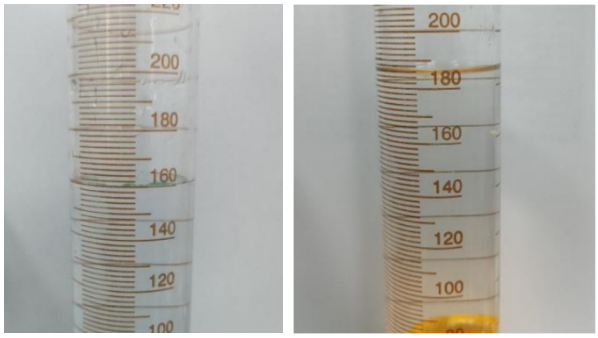

(a) Volume before starting (b) Volume added to the peel

Figure 8. Fresh tangerine peel volume

(4) Drying energy consumption

The power consumption during drying is recorded by using a pcolor power metering socket, as shown in Figure 9.

(a) Hot air 30℃ energy consumption (b) infrared hot air 35℃ energy consumption

Figure 9. energy consumption measurementt

The energy consumption measurement results are shown in Table 5.5. As temperature increases, power consumption decreases. Although the heating process requires higher power, the drying time is significantly shortened, resulting in reduced energy consumption. Overall, infrared drying consumes less energy than hot air drying, with energy savings of 18.18%,20.50%, and 22.56% at the same temperature. This study designed an intelligent temperature control system for infrared hot air drying equipment, which can adjust parameters such as infrared radiation intensity, hot air temperature, and airflow velocity in real-time based on material dryness levels, thereby enhancing drying efficiency and energy conservation.

4. Conclusion

This study developed an infrared hot air drying control system utilizing combined thermal infrared technology. Employing Mitsubishi PLC as the main controller, we designed both hardware and software for the drying chamber. Comparative tests demonstrated that while both systems exhibited comparable temperature regulation capabilities, the infrared hot air drying chamber showed shorter processing times, lower non-uniformity coefficients, reduced shrinkage rates, decreased energy consumption, and superior dried tangerine peel performance compared to electrically heated constant-temperature drum dryers.

References

[1] Zhu Kaiyang, Ren Guangyue, Duan Xu et al. Application of infrared radiation technology in drying of agricultural products [J]. Food and Fermentation Industry, 2021,47(2 0):303-311.

[2] Hu Zhonghuan, Yang Mingjin, Yang Zhuoran, et al. A heat drying model based on multi-physical field coupling and its verification [J]. Journal of Southwest University (Natural Science Edition), 2020,42(02):118-128.

[3] Ning Yangyang, Zhu Wenxue, Bai Xiting, et al. Effects of hot air-infrared segmented combined drying on the quality of shelled fresh peanuts [J]. Food and Fermentation Industry, 2024,50(04):133-142.

[4] Fan Yuhang, Wu Jinji, Song Weidong et al. Design and test of a combined system for dehumidification and hot air drying using super-dry film on melon seeds [J]. Journal of Agricultural Machinery Chemistry, China, 2025:126-131.

[5] Qu Wenjuan, Fan Wei, Ma Hailuo et al. Walnut drum catalytic infrared-drying and hot air drying test and energy consumption analysis [J]. Food and Machinery, 2021,37(05):163-168,193.

[6] Bie Yu, Zheng Siming, Chen Fei et al. A heat air circulation drying chamber with uniform flow field and its adjustment method [P]. Yunnan Province: CN20161003 6234.0, 2017-12-22.

[7] Mu Jinping, Zhou Jiachun, Jiang Lihua et al. Study on the combined drying characteristics of apple slices with infrared hot air [J]. Food Industry Science and Technology, 2016,92-96,169.

[8] Tan Guo, Dong Lin. Flow field simulation and structural optimization of infrared-hot air dryer [J]. Sichuan Agriculture and Agricultural Machinery, 2024(06):34-36+40.

[9] Ling Jing, Zhang Nan, Du Dengrong, et al. Fuzzy PID Composite Temperature Control Design for Infrared Drying Ovens [J]. China Testing, 2024,50(02):172-179.

[10] Zhu Xuefei. Design and research of microwave drying chamber based on PLC control [J]. Modern Information Technology, 2020,4(09):26-28+32.

[11] Huang Jun. Research and Design of a Blower-Drying Cabinet Based on a Microcontroller [J]. Electronic Design Engineering, 2017,25(21):173-176.

[12] Wen Yongshuang, Wang Shijun, Wei Zhongcai et al. Design of automatic temperature and humidity control system for drying chamber [J]. Agricultural Mechanization Research, 2016,38(09):250-2 54.

[13] Qian Shanzhu, Nandi. Structural design of drying chamber for alfalfa solar drying system [J]. Agricultural Machinery Research, 2015,37(05):239-241.

[14] Liu Yan and Feng Aiguo. Design of automatic weighing system for electric heating air-drying oven [J]. Food Research and Development, 2013,34(19):130-132.

[15] Lin Hongju. Design of temperature control system for electric heating air-drying oven [J]. Agricultural Mechanization Research, 2011,33(08):168-171+183.

[16] Li Ping. Research on Intelligent Control System of Web Dryer Based on PLC [D]. Sichuan: School of Mechanical Engineering, Xihua University, 2023.

[17] DB4407/T 70-2021. Geographical Indication Products: Xinhui Citrus Peel [S]. Jiangmen Market Supervision and Administration Bureau, 2021.